Archiwum Instytutu Techniki Cieplnej Vol. **1** nr 1(2016) www.itc.polsl.pl/ArchiwumITC

Identification and modelling of blood flow processes in section of large blood vessel using hybrid Euler-Lagrange multiphase approach[1]

Artur Knopek[2]

Key words: aorta, CFD, blood flow, ANSYS Fluent, multiphase, DPM

Abstract

Computational fluid dynamics (CFD) in past known only in highly specialized technical engineering branch is nowadays one of main engineering tool in solving numerous complex problems in order to get crucial information and extend general knowledge in many fields. CFD allows to create new, more advanced systems and also optimize already created to enhance efficiency and/or reduce costs of production and operating. Actual situation demands from engineers to face difficult competition - fighting for minor fractions of efficiency due to construction and materials limitations. That operations do not concentrate only on that obvious disciplines like heat transfer, fluid dynamics or power-generation, but also new uncharted areas like automotive, chemical, aerospace, environmental engineering etc.

One of that innovative field of CFD application is bio-engineering. In medicine, computer simulations can provide necessary, life-saving information with no interfere in patient body (in vivo), that allows to avoid later complications, application collisions and dangerous unpredictable after-effects. What more in several cases, in vitro analyses cannot be used through to life threats of treatment.

The main objective of current project is to develop and test novel approach of accurate modelling of human blood flow in arteries.

Currently available research reports do not cover the spatial interaction of individual blood phases and walls of blood vessels. Such approach could significantly reduce accuracy of such models. Proper simulations enriches general knowledge with specific details which could be

[1] Research carried out under the project No 2014/13/B/ST8/04225 funded by National Science Center.

[2] This section was prepared as a Master Thesis project by Artur Knopek at Institute of Thermal Technology at Energy and Environmental Engineering Faculty of Silesian University of Technology, under supervision of Dr Ziemowit Ostrowski

crucial in early diagnosis of potential cardiac problems showing vulnerable zones (e.g. narrowed blood vessels). Such precise information are extremely difficult to obtain experimentally.

Apart from multiphase concept of the project (that is considering every component of blood as separate phase assigning exceptional properties to each of them and determines relations between them) special attention was paid to the realism of geometry - considering the real system of the aortic segment (part of ascending aorta, aortic arch and part of thoracic aorta) including bifurcations. In addition a pulsating blood flow is being considered and implemented using built in UDF (User Defined Function) functionality of CFD code.

1. Introduction

1.1 Main goal of project

The main objective of current project is to develop and test novel approach of accurate modelling of human blood flow in arteries.

Currently available research reports usually do not cover the spatial interaction of individual blood phases and walls of blood vessels. Such approach could significantly reduce model accuracy. Proper simulations enriches general knowledge with specific details which could be crucial in early diagnosis of potential cardiac problems showing vulnerable zones (e.g. narrowed blood vessels). Such precise information are extremely difficult to obtain experimentally.

1.2 Computational Fluid Dynamics and ANSYS CFD

The permanent development of the technique enabled applying numerical methods to wide range of applications, thanks to enhancing the possibility of modern computers. The appropriate equipment and software are capable to deal with complicated problems and make advanced simulations which could not be solved with analytical methods. However, numerical methods through the process of the discretization does not provide accurate calculated answer, but its approximation with accuracy balanced according to needs. Nowadays thanks to high computing power one can explore even so sophisticated field of life as bioengineering [8]. Usage of Computational Fluid Dynamics (CFD) solver [A] allows to assemble all essential information. A hybrid multifluid Euler-Lagrange approach is proposed in current study, being a part of wider research project targeted at modelling of blood flow in human artery section. Calculations was based on bundled software (ANYS Inc., USA) – highly developed engineering tool allowing to investigate problems with many approaches to get real behavior of blood flow (velocity, pressure, particles deposition etc.)

1.3 Concept of blood as a multiphase fluid

In proposed model, the multifluid [9] approach is used to model blood consisted of plasma and RBCs (Red Blood Cells) as interpenetrating phases. In addition, the leukocytes (which volume fraction is about 1% of the overall blood volume) are represented as dispersed phase. In proposed methodology, where collisions of WBCs (White Blood Cells) can be modeled, the advantages of hybrid Euler Lagrange [15] model are used.

The interaction between phases and within phases are calculated in Eulerian grid, where the calculated interaction stress tensor, is used by dispersed phase to take into account collision effect. As a result, the 3D structure of mutually interacting particles will be modelled.

1.4 Blood and geometry properties

Apart from multiphase concept of the project, that is considering every component of blood as separate liquid assigning unique properties to each of them and determines relations between them. Special attention was paid to the realism of geometry - considering the real system of the aortic segment (part of ascending aorta, aortic arch and part of thoracic aorta) including bifurcations. In addition, a pulsating blood flow was implemented with using a built in UDF (User Defined Function) module which will employ lumped model of human circulatory system.

2. Biomedical specifications

2.1 Basic definitions

Heart – muscular organ build of two chambers and two atria (right and left). Atria are separated from each other by interatrial septum and chambers by interventricular septum. Atria are separated from chambers by atrioventricular septum with two holes in it (left and right) with 2 cm diameter each. Chambers and atria works as a 4 series pumps (right chamber and atrium; left chamber and atrium) which supplies all human cardiovascular system. There is one direction of blood flow – from veins reservoir to aortic reservoir thanks to build of heart and existence of valves which prevents backflow of blood [17].

Cardiac cycle – consist of two phases: systole - period of cycle when chambers contracts and ejects part of contained blood to large aortic reservoirs and diastole - period of cycle when heart chambers muscles are under relaxation, pressure and blood fulfillment in them is lowering. Phases are repeated cyclically with frequency of 1,2Hz (72 times per minute). One cycle last about 800 ms (systole – 270ms; diastole – 530ms) [7].

Stroke Volume (SV) is the amount of blood pumped by heart chambers to specific aortic reservoirs. Every of each chamber pumps about 75 mL of blood in one cardiac cycle (adult male with total mass of 70 kg, in quiescence and lying position). At the end of cycle in heart remains about 50 mL of residual blood volume, which conditions end-systolic ventricular volume [17].

Heart work – in physic work (W) is the force (F) working on the certain distance (L)

$$W = F \cdot L \tag{1}$$

Essential feature of heart is volume of ejected blood and pressure in aorta, which heart must overcome to pump mentioned amount and accelerate it to required speed. There is an external and internal work of heart. Internal responds for contraction tension generation, while external responds for pumping blood. Total heart energy W_t consist of energy necessary to sustain pressure in blood vessels – potential energy (E_p), energy necessary to accelerate blood flow after its been pump from heart to vessels – kinetic energy (E_k), energy necessary to overcome gravitation force (E_g).

$$W_t = E_p + E_k + E_g \tag{2}$$

In normal conditions E_k is equal to 5% of total energy and is feasible to calculate it by equation:

$$E_k = \frac{m \cdot v^2}{2} \tag{3}$$

where: m – mass, kg; v – velocity, m/s;

Potential energy is equal to 95% of total energy and is feasible to calculate it by eq. (4):

$$E_p = P_A \cdot V_s \tag{4}$$

where: P_A- pressure in arteries, Pa; V_s- stroke volume, m^3;

2.2 Large Blood Vessel – Aorta

Vascular system is a systemic arterial reservoir which includes: aorta, arteries, arteriole, capillaries, wenule and veins. Main function of the aorta, arteries and arteriole (fig.2.1) is blood transport under high pressure to tissue and changing of pulsatile flow to continuous flow. Aorta leaves from the left chamber of a heart and subdivide to: ascending aorta, arch of aorta with bifurcations, descending aorta which divides to the thoracic and the abdominal aorta [10].

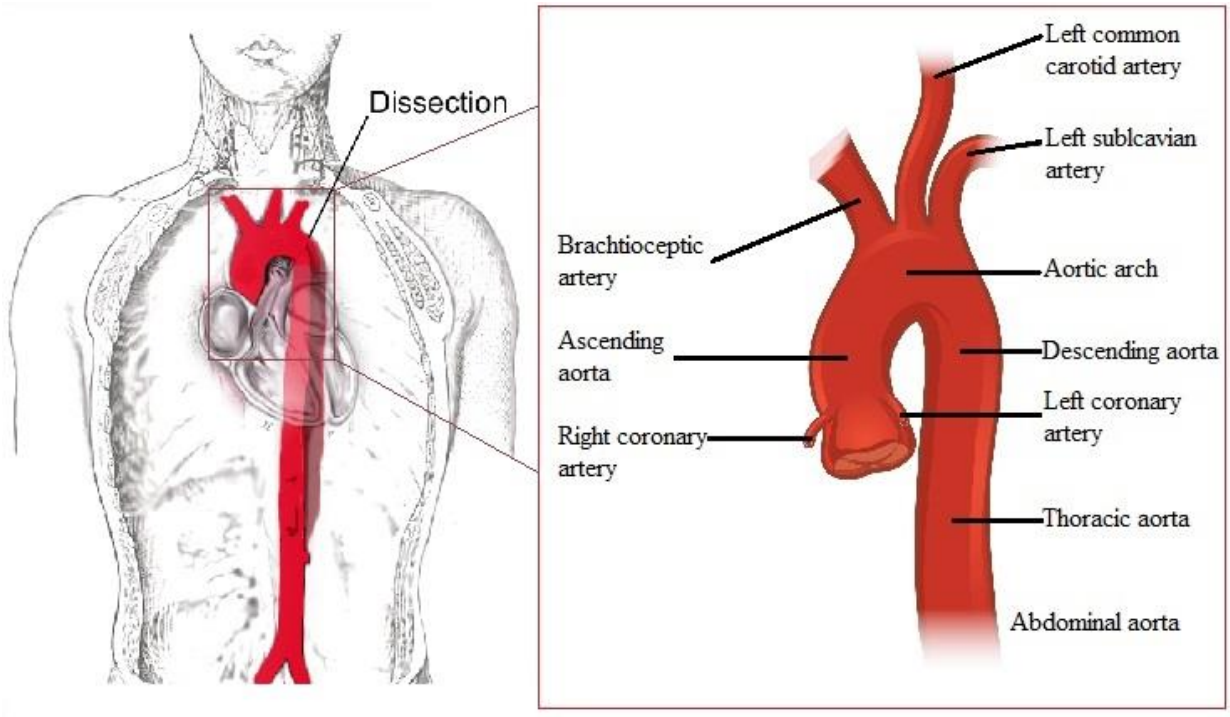

Fig.2.1. Aorta placement in human body (left[3] and right[4])

[3] Creative Commons Attribution-Share Alike 3.0 Unported. After author: Fvasconcellos. Image: AoDissekt_scheme_StanfordB.png by JHeuser; https://commons.wikimedia.org/wiki/File:AoDissekt_scheme_StanfordB_en.png#filelinks

[4] Creative Commons Attribution 3.0 Unported. After author: OpenStax College; https://commons.wikimedia.org/wiki/File:2121_Aorta.jpg

Arterial flow characterized by: pressure, velocity of blood flow, capacity, arterial pulse. Arterial reservoir contains about 550 mL of blood, what is about 11% of all blood flowing in human organism. Cardiac output is in quiescence about 0,9 l/min. The same amount of blood must flow in aortic, arteries, arterioles etc. cross sections, causing gradual enlarging of summary cross section which must be supplied with blood. Due to that velocity of blood is lowering, referring to the equation [10, 17]:

$$v = Q / \sum A \tag{5}$$

where: v – velocity, m/s; Q – blood flow, kg/s; A – summary area of cross sections, m^2;

The biggest summary cross section area is in capillaries where velocity in quiescence is the lowest – almost 0. In common adult aorta, which cross section is about 4,5 cm^2 and total maximum flow about 0,2 l/s, velocity is about:

$$v_A = \frac{0{,}2\ dm^3/s}{0{,}045\ dm^2} = 4{,}44\frac{m}{s} \approx 16\frac{km}{h}$$

Arterial blood pressure depends on inflow and outflow from arterial reservoir. When inflow and outflow is stabilized and there is no change in walls tension of aorta, average pressure in that reservoir do not change and depend on cardiac cycle. For maximum ejection of left chamber pressure is the highest (systolic arterial pressure) and its equal to 16 kPa (120 mm Hg), when the diastolic arterial pressure is the lowest and equal to 9,3 kPa (70 mm Hg) [17].

2.3 Blood components

Blood is a liquid tissue, filling bloodstream, separated from other organism tissues with a layer of endothelium with total area of about 100m^2. Blood is in constant flow and comprise 6-7% of total human mass. Blood consist of blood cells which is about 45% of blood volume (leukocytes, erythrocytes, thrombocytes) and plasma [10].

Plasma is partially transparent, pale straw (yellow) colored liquid, iridescent fluid, which mostly consist of water (90-92%) and contains dissolved organic and nonorganic proteins [7]. Density of plasma is equal to 1022 – 1026 kg/m^3.

Erythrocytes (Red Blood Cells) are produced by bone marrow. Their main purpose is transporting oxygen along the organism. Theirs unique shape connected with flexibility is highly important in that proses. Average diameter of one RBC is about 8 μm and its round, biconcave disc (Fig.2.1), its area equals to 120μm. The amount of RBCs in 1μl of blood is about 5mln in men and 4,5mln in women, density is equal to 1095 – 1101 kg/m^3 [7].

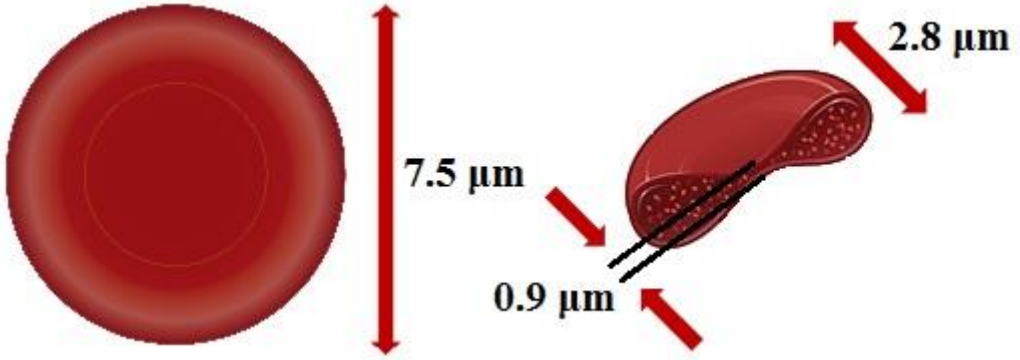

Fig.2.1. RBCs structure (left[5] and right[6])

Hematocrit (Hct) is crucial parameter (6) describing volume of RBCs (V_{RBCs}) ratio to total blood volume (V_B). It has significant influence on numerous blood parameters. Usually in percentage 45% for men and 40% for women.

$$Hct = \frac{V_{RBCs}}{V_B} \cdot 100\% \qquad (6)$$

2.4 Leukocytes

Mainly function of WBCs is to defend the organism from pathogenic germs. The amount of WBCs in 17,5 µml of blood is about 4000 – 11000 what gives amount less than 1% in total blood volume. Divided on many different kinds (tbl.2.2), it is possible to specify them by structure on two main groups granulocytes (presence of granules in its cytoplasm) or agranulocytes (absence of granules in its cytoplasm) [7].

Tbl.2.2. Chosen characteristic feature of WBCs

Type		Amount in 1l of blood · 10^9	Approx. %	Diameter µm
Granulocytes	Neutrophil	4,4	62	10-12
	Eosinophil	0,2	2,3	10-12
	Basophil	0,04	0,4	10-15
Lymphocyte		2,5	30	8-9
Monocyte		0,3	5,3	15-30

[5] Creative Commons Attribution-Share Alike 4.0 International. After author: Cancer Research UK uploader; https://commons.wikimedia.org/wiki/File:Diagram_of_a_red_blood_cell_CRUK_467.svg

[6] Creative Commons Attribution-ShareAlike License. After author: NHLBI; https://commons.wikimedia.org/wiki/File:Modified_sickle_cell_01.jpg

3. Numerical model

3.1 General information about CFD

Computational fluid dynamics (CFD), [8] in past known only in highly specialized technical engineering branch, is nowadays one of main engineering tool in solving several complex problems in order to get crucial information and extend general knowledge in many fields. CFD allows to create new, more advanced systems and also optimize already created to enhance efficiency and/or reduce costs of production and operating. Actual situation demands from engineers to content with difficult competition - fighting for percentage of efficiency due to construction and materials limitations. Operations not concentrates only on that obvious disciplines like heat transfer, fluid dynamics or power-generation, but also new uncharted areas like automotive, chemical, aerospace, environmental engineering etc.

One of that innovative field of CFD application is bio-engineering [16]. In medicine, computer simulations can provide necessary, life-saving information with no interfere in patient body (in vitro), allowing to avoid later complications, application collisions and dangerous unpredictable after-effects. What more in several cases in vitro analyses can be impossible to use through to life threats of treatment.

3.2 Finite volume method

The FVM is main discretization model in ANSYS Fluent. Domain is subdivided on finite control volumes called cells. Mesh (set of cells) allows program to obtain continuous calculation of momentum exchange law through domain. Program uses the cell-centered (CC) method for calculating conservation equations – whole cell value is equal to its center (fig.3.1). First, average values of chosen parameters are stored in the centroids and then, discrete equations of conservations laws are calculated in order to obtain whole value of all volume (cell). Methods used to calculate average values of the centroids are described in section 3.8. [13]

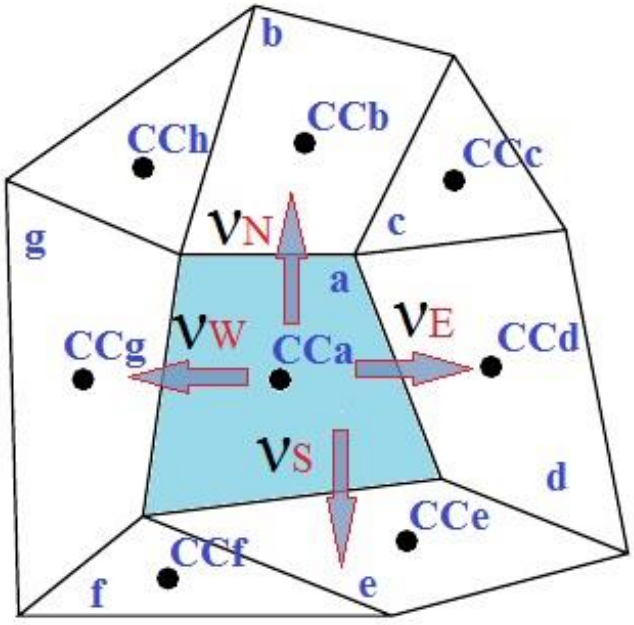

Fig.3.1. Presentation of Cell Centered Finite Volume Method

3.3 Euler – Euler Approach

In Eulerian approach, the base characteristic of the solid phase is calculated as a continuous medium with main properties assumed as dispersed phase of fluid - and is treated as a continuum. Important feature of mixture consisting of two fluids is individual fraction volume concentration. To obtain phases transport equations terms of fluid continuity and momentum conservation must be provided. It is impossible to consider every point of time and space of the two continua flow. Therefore conservation laws are solved separately and then combined in discretized geometry, taking in account volume concentration of each phase [3].

3.3.1 Specific project usage

Eulerian approach was used in calculations of interactions with diffused phases and within phases of plasma and erythrocytes. Assumption of granular second phase in multiphase model [A] requires to define flow as a solid-fluid mixture. for the case where assumption of inelastic granular phase is used, it is necessary to found the combination of the random molecules motion among particles collisions and thermal motion of particles in a fluid when calculating solid phase stresses. Pressure, stresses and viscosity of the solid phase are determined by intensity of molecules velocity fluctuations. Therefore it is necessary to implicate particle velocity fluctuations (which is a result of particle kinetic energy) with granular temperature (equal to random particle motions mean square).

The general momentum conservation law includes interactions between more than two phases. In this case main phase law (fluid) is shown in (7), when the second phase in (8) including exchange of moment between main and secondary phase.

$$\frac{\partial\left(\rho_f \varepsilon_f \overrightarrow{v_f}\right)}{\partial t} + \nabla \cdot \left(\rho_f \varepsilon_f \overrightarrow{v_f}\overrightarrow{v_f}\right) = \rho_f \varepsilon_f \vec{g} - \varepsilon_f \nabla P_f + \nabla \cdot \overrightarrow{\overrightarrow{\tau_f}} + K_{sf}\left(\overrightarrow{v_s} - \overrightarrow{v_f}\right) \tag{7}$$

$$\frac{\partial(\rho_s \varepsilon_s \overrightarrow{v_s})}{\partial t} + \nabla \cdot (\rho_s \varepsilon_s \overrightarrow{v_s}\overrightarrow{v_s}) = \rho_s \varepsilon_s \vec{g} - \varepsilon_s \nabla P_f - \nabla P_s + \nabla \cdot \overrightarrow{\overrightarrow{\tau_s}} + K_{fs}\left(\overrightarrow{v_f} - \overrightarrow{v_s}\right) \tag{8}$$

where: f – fluid phase; s – solid phase; $\vec{g}$ – gravitational acceleration, m/s^2; $\vec{\vec{\tau}}$ – stress tensor, N/m^2; P_s - granular pressure, Pa; P_f – fluid pressure, Pa; ρ_s – solid density, kg/m^3; $\overrightarrow{v_{s/f}}$ – solid/fluid velocity, m/s; t – time, s; K – interphase exchange momentum coefficient

3.3.2 Interphase exchange momentum coefficient (General Model)

One of the crucial implementation in conservation law [A] is interphase exchange momentum coefficient which determines behavior of phases in domain. Interphase exchange momentum coefficient general model equation is presented below.

$$K_{fs} = \frac{\varepsilon_s \rho_s f}{\tau_{rel}} \tag{9}$$

where: f – drag function, τ_{rel} – particulate relaxation time, s;

$$\tau_{rel} = \frac{\rho_s d_s^2}{18\mu_l} \tag{10}$$

where: d_s –diameter of solid particle, m; μ_l – viscosity of liquid phase, Pa·s;

3.3.3 Drag model - Gidaspow

Different models formulates *f* function in other way usually using the drag coefficient C_D (based on the Reynolds number). To calculate momentum exchange within RBC's and Plasma Gidaspow [5] model approach was used. General assumption of models are:

Drag function must be multiplied by main phase volume fraction to obtain no momentum exchange if there is no main phase, there is no momentum exchange and the only determinant is fractions volume.

Gidaspow model approach highly depends on volume fraction by using two different equations: Wen and Yu (11) [18] or Ergun equation (12) [4]. Momentum exchange coefficient K_{fs} equates:

when $\varepsilon_f > 0{,}8$ (Wen and Yu):

$$K_{fs} = \frac{3}{4} C_D \frac{\varepsilon_s \varepsilon_f \rho_f \left|\overrightarrow{v_s} - \overrightarrow{v_f}\right|}{d_s} \varepsilon_f^{-2{,}65} \tag{11}$$

when $\varepsilon_f \leq 0{,}8$ (Ergun):

$$K_{fs} = 150 \frac{\varepsilon_s (1 - \varepsilon_f) \mu_f}{\varepsilon_f d_s^2} + 1{,}75 \frac{\rho_f \varepsilon_f \left|\overrightarrow{v_s} - \overrightarrow{v_f}\right|}{d_s} \tag{12}$$

where C_d is calculated from (13):

$$C_D = \frac{24}{\varepsilon_f Re_s} \left[1 + 0{,}15 (\varepsilon_f Re_s)^{0{,}687}\right] \tag{13}$$

Where:

Re - relative Reynolds number, presented in equation below

$$Re_s = \frac{\rho_f d_s \left|\overrightarrow{v_s} - \overrightarrow{v_f}\right|}{\mu_f} \tag{14}$$

Project assumes constant RBC's fraction volume ε_s for about 44% of total flow volume what had an effect in usage mostly Erguns equation.

3.4 Standard $k - \varepsilon$ model

Assumption of turbulent standard k - ε model was made in which transport equations are calculated separately: k – turbulent kinetic energy and ε – rate of dissipation. By coupling exact equations of (k) and partially empirical equations of (ε) model received acceptable accuracy in large range of turbulent flows which occurred in studied case. Equations calculated per phase are presented below in (15) and 16) [11]:

$$\frac{\partial}{\partial t}(\rho k) + \frac{\partial}{\partial x_i}(\rho k u_i) = \frac{\partial}{\partial x_j}\left[\left(\mu + \frac{\mu_t}{\sigma_1}\right)\frac{\partial k}{\partial x_j}\right] + S_k + S_b - \rho\varepsilon - G_M \tag{15}$$

and

$$\frac{\partial}{\partial t}(\rho\varepsilon) + \frac{\partial}{\partial x_i}(\rho\varepsilon u_i) = \frac{\partial}{\partial x_j}\left[\left(\mu + \frac{\mu_t}{\sigma_2}\right)\frac{\partial \varepsilon}{\partial x_j}\right] + G_1\frac{\varepsilon}{k}(S_k + G_3 S_b) - G_2\rho\frac{\varepsilon^2}{k} \tag{16}$$

where:
S_k - turbulence kinetic energy generation due to the mean velocity gradients, J/kg; S_b - turbulence kinetic energy generation due to buoyancy, J/kg; G_M - contribution of the fluctuating dilatation in compressible turbulence to the overall dissipation rate, J/kg.

Eddy viscosity μ_t is calculated from (17).

$$\mu_t = \frac{k^2}{\varepsilon}\rho G_\mu \tag{17}$$

Constants G_1, G_2, $G_3, G_\mu, \sigma_1, \sigma_2$ used in above equations are empirical values obtained from experiments and observations founded to work properly in practical engineering.

3.5 Partial Differential Equation - Granular Temperature Model

The granular temperature θ_t of the solid phase in the Euler approach is proportional to the kinetic energy of the random motion of the particles and is calculated from (18):

$$\theta_t = \frac{1}{3}u_{S,j}u_{S,j} \tag{18}$$

where:
$u_{S,j}$ - Cartesian coordinates (j) of the fluctuating solid (S) velocity

While the transport equation [2] as (19):

$$\frac{3}{2}\left[\frac{\partial}{\partial t}(\rho_s\varepsilon_s\theta_t) + \nabla\cdot(\rho_s\varepsilon_s\overrightarrow{v_s}\theta_t)\right] = \left(-p_s\bar{\bar{I}} + \bar{\bar{\tau}}_s\right):\nabla\overrightarrow{v_s} + \nabla\cdot\left(k_{\theta_t}\nabla\theta_t\right) - \gamma_{\theta_t} \tag{19}$$

where:
$\left(-p_s\bar{\bar{I}} + \bar{\bar{\tau}}_s\right):\nabla\overrightarrow{v_s}$ - generation of energy by the solid stress tensor, J/kg;
γ_{θ_t} - the collisional dissipation of energy, J/kg; $k_{\theta_t}\nabla\theta_t$ - the diffusion of energy (k_{θ_t} is the diffusion coefficient), J/kg.

For obtaining k_{θ_t} Gidaspow et al. model was assumed [6] and calculated (20):

$$k_{\theta_t} = \frac{150\,\rho_s d_s\sqrt{\theta\pi}}{348(1+e_{ss})g_{0,ss}}\left[1 + \frac{6}{5}\varepsilon_s g_{0,ss}(1+e_s)\right]^2 + 2\rho_s{\varepsilon_s}^2 d_s(1+e_{ss})g_{0,ss}\sqrt{\frac{\theta_t}{\pi}} \tag{20}$$

where:

$g_{0,ss}$ - radial distribution function; e_{ss} – solid-solid restitution coefficient; e_s - solid restitution coefficient,; γ_{θ_t} - collisional dissipation of energy, J/kg.

Energy dissipation within the solids phases as a result of interparticle collisions and is equal to (Lun et al.) [12]:

$$\gamma_{\theta_t} = \frac{12(1+{e_{ss}}^2)}{d_s\sqrt{\pi}}\rho_s{\varepsilon_s}^2{\theta_t}^{1,5} \tag{21}$$

3.6 Euler – Lagrange Approach

Lagrange approach describes particle trajectory which has momentum, mass and energy. Particle is tracked in moving coordinate frame following the particle in time (22) [3]:

$$V = V(x,y,z,t) \tag{22}$$

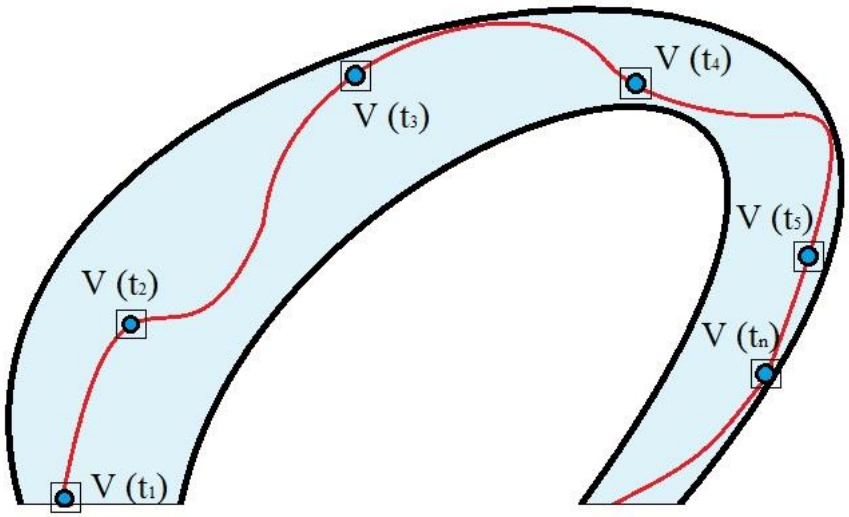

Fig.3.2. Particle streamline in domain

ANSYS Fluent [A] combines both of approaches (Eulerian, Lagrangian) by calculating Eulerian phases as a continuum, using Navier-Stokes equations. Dispersed phase as a dependent numerous particles flowing though calculated flow field (Eulerian grid) and exchanging momentum, mass, and energy with the main phase. Euler – Lagrange approach in hybrid model allows to obtain all crucial information about blood behavior (e.g. velocity vectors, pressure distribution, particles positions in blood vessel)

Change of dispersed phase momentum is calculated from (23):

$$F = \sum\left(\frac{18\mu C_D Re}{\rho_p d_p^2 24}\left(u_p - u\right) + F_o\right)\dot{m}_p\Delta t \tag{23}$$

where:

μ – fluid viscosity, Pa·s; ρ_p – particle density, kg/m^3; d_p – particle diameter, m; Re – Reynolds number; u_p – particle velocity, m/s; u – fluid velocity, m/s; C_D – drag coefficient, $\dot{m}_p$ – mas flow rate of particles, kg/s; Δt – time step, s; F_o – other forces

Drag coefficient C_D, for smooth particles equals to

$$C_D = \alpha_1 + \frac{\alpha_2}{Re} + \frac{\alpha_3}{Re^2} \tag{24}$$

Where $\alpha_{1,2,3}$ are constants related to Re numbers Given by Morsi and Alexander [14].

3.7 Particle injection

The *Particle Type* was chosen as inert. Moreover, the surface injection type was determined as particle stream releasing particles from each cells face on chosen boundary condition. The particle injection visualization is presented in (Fig.3.3).

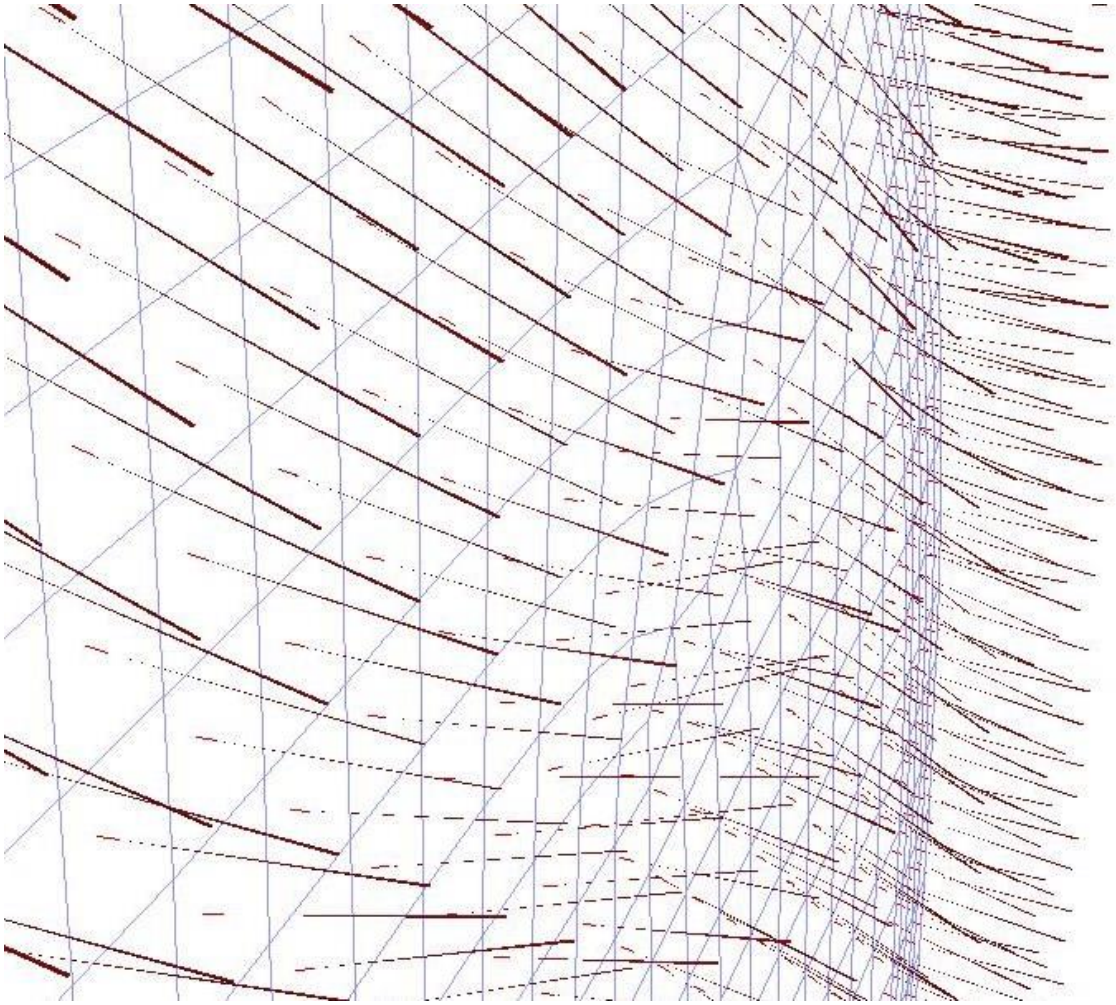

Fig.3.3. Injecting particles parcels from faces

In chosen approach, momentum equation is not calculated for an individual particles [1]. Program mechanism for tracking is based on parcels – groups of particles. Particles in each parcel have equal value of main properties (position, mass, velocity). Number of particles in parcel depends on individual particle mass and can be obtained from (25):

$$n_p = \frac{\dot{m}_p}{m(d,\rho)}\Delta t \tag{25}$$

where: Δt - time step, s; $\dot{m}_p$ - single parcel source mass flow rate, kg/s; m - mass of an individual particle, kg; d - particle diameter of an individual particle, d; ρ – density of an individual particle, kg/m^3.

3.8 Rosin-Rammler Diameter Distribution Method (RRDDM)

To better represent the variation of leukocytes diameters, RRDDM was used [A]. Full range of available diameters (continuous function) is divided on narrow intervals. Representation of each interval is its mean diameter injected as a separated stream. If particle diameter is > d, mass fraction is calculated from (26):

$$Y_d = e^{-(\frac{d}{\bar{d}})^n} \tag{26}$$

Y_d – mass fraction, kg; d – droplet diameter, m; $\bar{d}$ – size constant – mean diameter, m; n - size distribution parameter – spread parameter.

According to paragraph 2.6, the largest part of WBSs are neutrophils what determinates choosing its diameter as a general mean diameter of a model (Table 3.1).

Specific values of diameter distribution parameters used in RRDDM for obtain acceptable diversity of WBCs are shown in tbl.3.1:

Table.3.1. RRDDM characteristic parameters

Parameter	Value
Max diameter	15 μm
Mean diameter	11 μm
Min diameter	7 μm
Spread	8
Number of Diameters	6

3.9 Green-Gauss Node-Based Gradient Evaluation (G-GN-B)

To obtain scalar value on cells' faces, secondary diffusion terms and velocity derivatives are necessary to calculate gradients [A]. Gradients are important part of conservation equations (in discretization of diffusion and convection condition):

$$\bar{\varphi}_{fc} = \frac{1}{N_{fc}} \sum_{n}^{N_{fc}} \bar{\varphi}_n \tag{27}$$

where:

φ_{fc} – value of φ at the cell face centroid, $\bar{\varphi}_{fc}$ – arithmetic average of the nodal values on the cells faces, $\bar{\varphi}_n$ – nodal values constructed from the weighted average of the cell values surrounding the nodes, N_{fc} – number of nodes on face.

Node-based gradient scheme is more accurate than cell-based on skewed and distorted meshes but may be more computational expensive

4. Model properties

4.1 Discrete Phase Model (DPM)

Discrete phase model is a practical answer of ANSYS Fluent for Lagrangian reference frame. Model ignores inner-phase, particle-particle impact with assumption that discrete phase has a low volume fraction according to main phase. However, high mass loading in model is possible. Trajectories of dispersed phase particles are calculated separately in chosen steps. Model calculations were synchronized with general frame time step. Computations of DPM were made at the beginning of iteration proses based on previous step calculations. No particles at the beginning of simulation was assumed. Injection begins in first time step. The amount of WBCs is a percentage mass fraction of the continuous phases (RBCs + Plasma) and it is equal to 1%.

WBCs are threated similarly to RBCs – like a granular suspension in plasma. The difference is (despite of total volume WBCs fraction which is negligible) that Leukocytes do not exchange momentum with main phase but are carried without any influence on main phase [A].

4.2 Geometry

Geometry used in the model was obtained from CFD Challenge [C] and presents real geometry adopted from 8-year old female patient MRA imagining (Gadolinium-enhanced Magnetic Resonance Angiography), performed using 1.5-T GE Signa scanner. The model geometry is presented in (fig.4.1). Patient had congenital defect of cardiovascular system – Coarctation of the aorta (CoA) which was about 65% of the blood vessel cross-section area reduction. Examined regions were: ascending aorta (AAO), aortic arch with bifurcation - innominate artery (IA), left common artery (LCCA), left subclavian artery (LSA) and descending aorta (DAO).

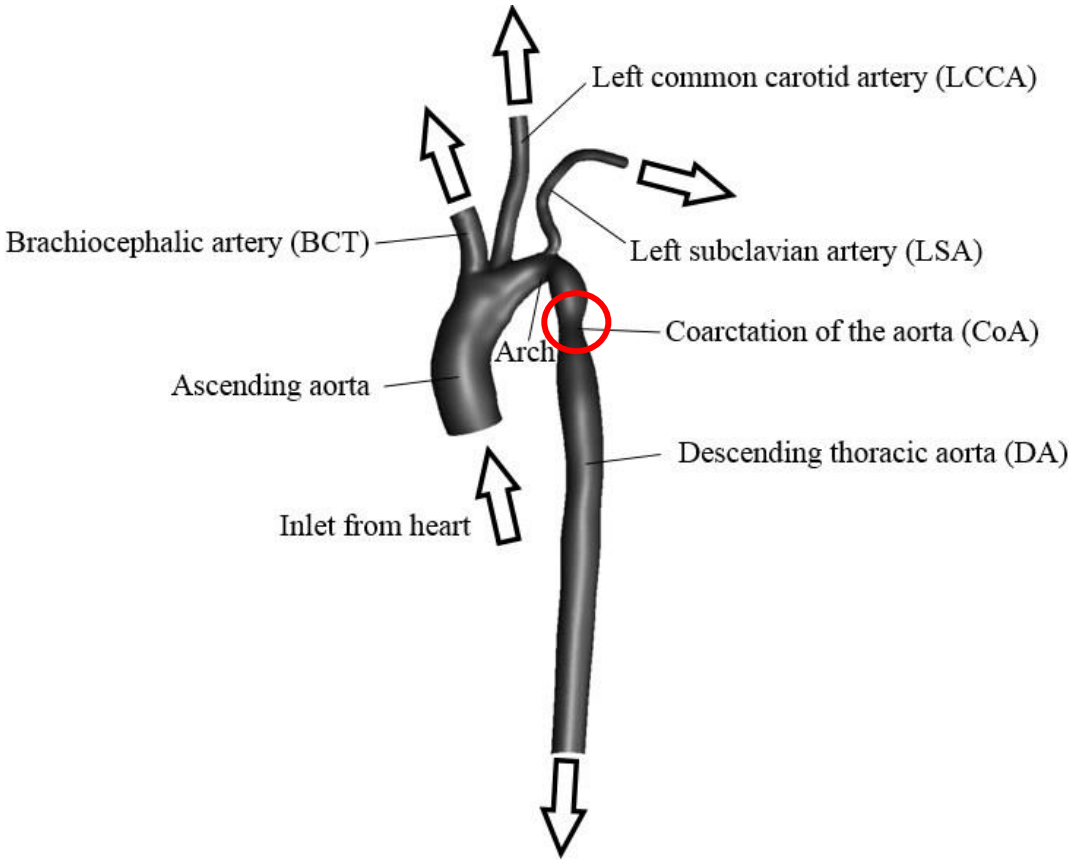

Fig.4.1. Geometry of the model used in the numerical simulations.

4.3 Boundary Conditions

The importance and difficulty of proper setting the BCs (*boundary conditions)* is one of the key feature in CFD modeling process. Used geometry demands well adaptation of 5 BCs - one inflow and four outflow. Ansys Fluent [A] determinates restrictions and limitations regarding to boundary conditions due to them not all of inlet-outlet relations are compatible. When considered domain has a multiple outlets, the recommended outlet boundary condition is OUTFLOW what reduce possible inlet conditions to velocity inlet condition only.

4.3.1 Inlet BC

At inlet to domain in Fig.4.1 *Inlet from heart* modeled BC was **velocity inlet**. To obtain more realistic behavior of human cardiovascular model pulsatile flow was implicated. Data was obtained from CFD Challenge in which blood flow was measured using phase-contrast (PC) cine sequence with through-plane velocity encoding [C]. The measured (shown in Table 4.1) blood flow presented is in time dependent points of cardiac cycle which was assumed as 0,7s. In effect volumetric flow was obtained. Due to chosen inlet BC volumetric blood flow was recalculated basing on stream continuity equation (4.1). To get constant blood flow in cardiac cycle data was interpolated within chosen periods of time to derive interpolation functions.

$$V(t) = Av \tag{4.1}$$

Tbl.4.1. Time dependent mass flow measurement and velocity

T	mm^3/s	m/s
0	3214,5	0,0157
0,035	12736,1	0,0623
0,07	70423	0,3445
0,105	171359,4	0,8382
0,14	201975,2	0,9880
0,175	176127,7	0,8616
0,21	141663,4	0,6930
0,245	100536,8	0,4918
0,28	73060,3	0,3574
0,315	36444,2	0,1783
0,35	10113	0,0495
0,385	**-257,1**	**-0,0013**
0,42	6611,8	0,0323
0,455	14545,6	0,0712
0,49	21754,2	0,1064
0,525	18761,3	0,0918
0,56	13006,3	0,0636
0,595	3472,9	0,0170
0,63	2223,4	0,0109
0,665	4190,7	0,0205
0,7	3214,5	0,0157

Highlighted (bold) characteristic measure point shows common occurring in heart process of blood backflow, which was zeroed (essential negative influence on model stability with outflow BC).

Effect of undertaken operations is shown in Figure 4.2, where two characteristic periods are specified: systole (when the left heart ventricle contracts, and blood flows to the aorta with maximum speed) and diastole (when the semilunar valve is closed, the atrioventricular valves are open, and the whole heart is relaxed).

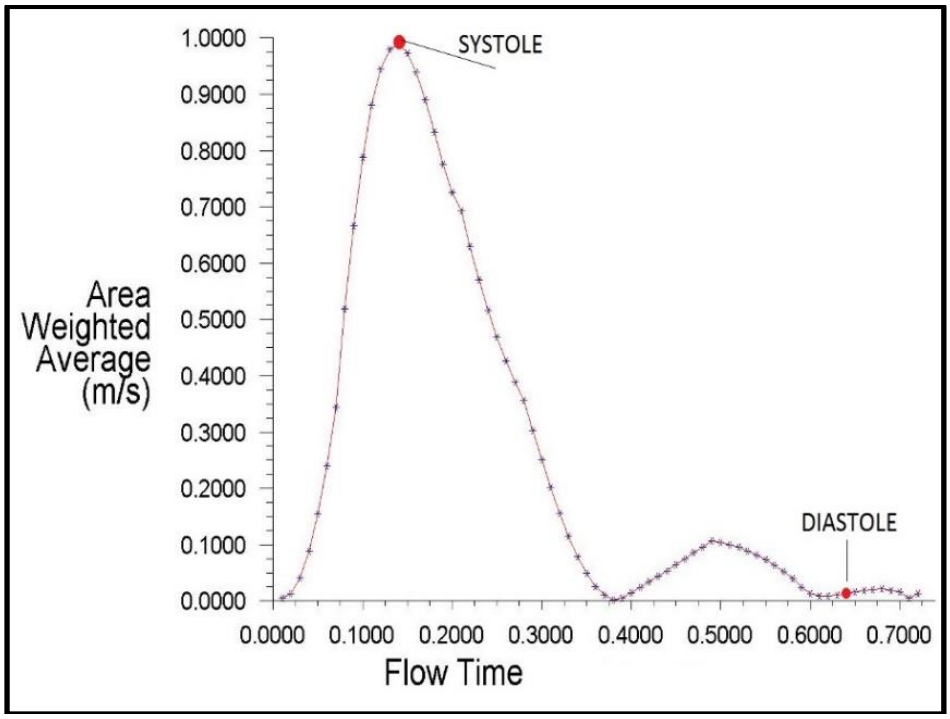

Fig.4.2. Inlet velocity obtained in model

Implication of the inlet pulsatile flow was possible with usage of UDF (*User Define Function*) – special feature in ANSYS products allowing to adjust program standard commercial code features and options in order to get more advantageous results. Periodic flow is obtained through time dependence of auto-implicated flow velocity in every repeatable cycle. UDF uses particular internal functions based on C# programming language.

Fraction percentage share on inlet assumed in model is 44% of RBC and its complement equal to 56% is Plasma.

4.4 Outlet BC

As said in previous paragraph BC appropriate in chosen system is **Outflow**, which is used to calculate model flow exits if pressure and velocity magnitude is unknown. Outflow BC was chosen in all outlets (BCA, LCCA, LSA, DA – cf. Fig. 1). Amount of fluid volume leaving domain depends percentage on inlet flow volume and its shown in Table 4.2.

Tbl.4.2. Outlet boundary conditions fractions distribution

Outlet Surface	Fraction, %
Brachiocephalic artery (BCT)	25,6
Left Common Carotid Artery (LCCA)	11,3
Left Subclavian Artery (LSA)	4,3
Descending aorta (DA)	58,8

4.5 Blood properties used in model

Taking in account blood phases it is necessary to show implemented values in model (tbl.4.3)

Tbl.4.3. Modeled blood parameters

Plasma density, kg/m^3	1026
Plasma viscosity, Pa·s	0,0035
RBC density, kg/m^3	1101
RBC viscosity, Pa·s	0,00417
WBC density, kg/m^3	1125

4.6 Mesh

One of inherent element of CFD modeling is the discretization of the domain. Not only mesh element quality is crucial but also mesh element size must be adjusted to selected timestep. Optimum mesh element size is obtained when particles flow thru subsequent cells without passing any of them (causing information loos and inaccuracy). Second limitation is not to calculate the same particle multiple times in one control volume in order to overburden the computing power.

In the thesis, hybrid mesh was created with approximately 720 000 elements (hexagonal, tetrahedral) (fig.4.4). Hexagonal part situated on inlet and descending aorta was created in order to better track discrete phase elements. In parts when intensive fluctuation occurs mesh was desilicated to avoid numerical errors (aortic arch). More precise view on inlet and outlet is presented in Fig. 4.3, showing inflation of mesh near boundaries.

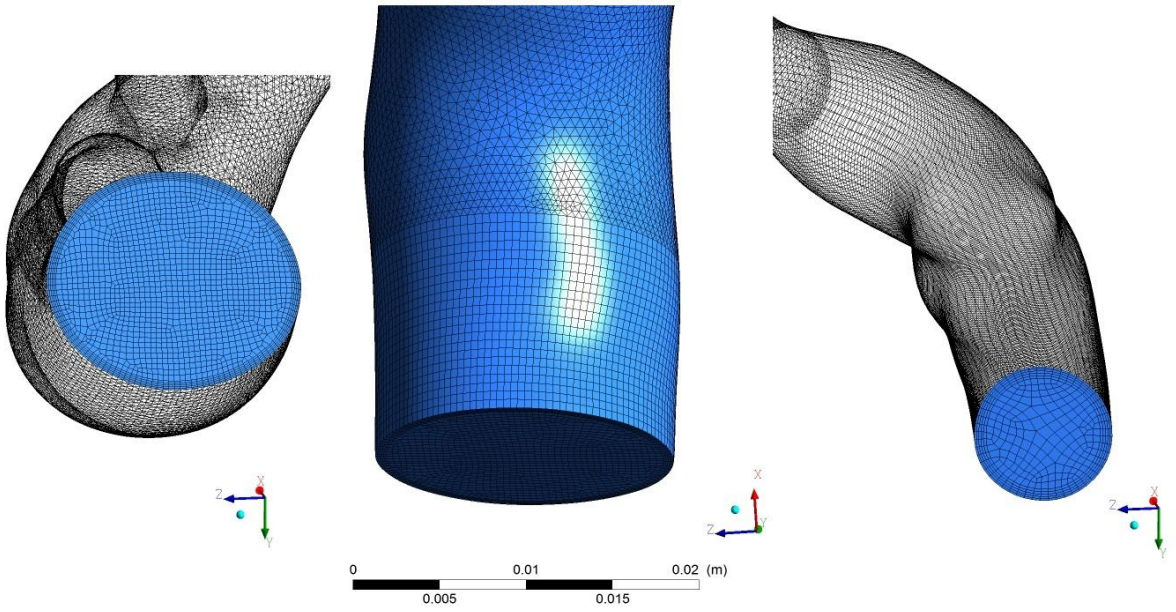

Fig. 4.3. Precise insight on inlet and outlet mesh

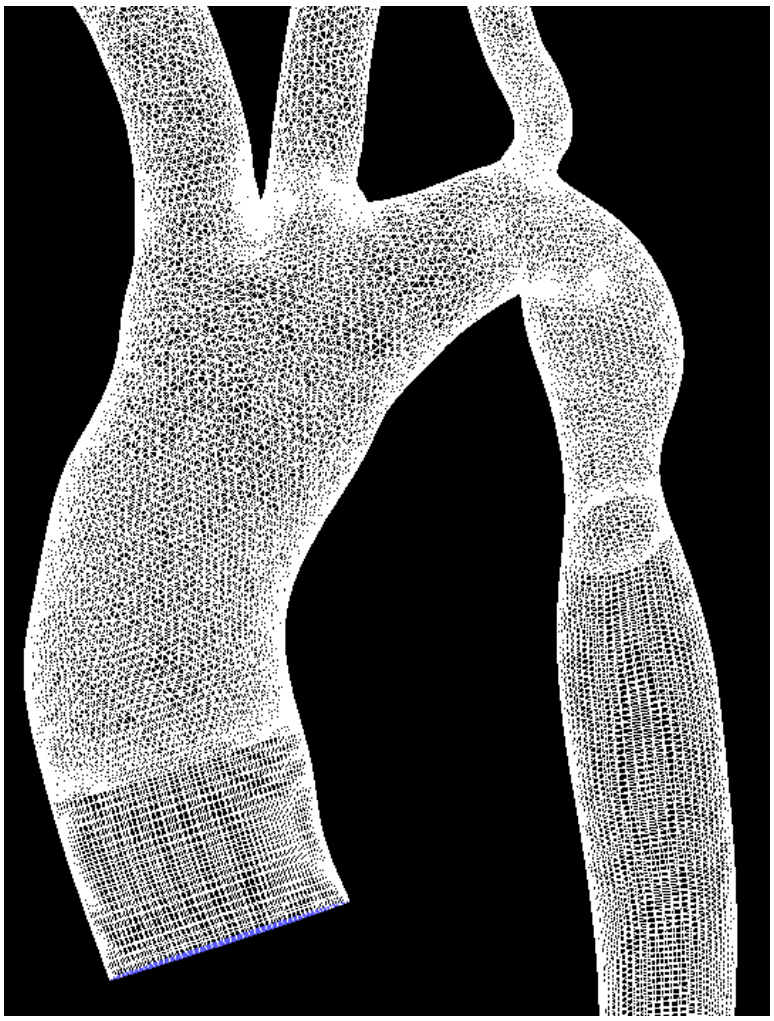

Fig.4.4. Hybrid mesh

5. Results

Calculation was made on 3D model with rigid walls presented in section 4. Transient simulation was performed with timestep $\Delta t = 0{,}01$. Operating fluid was incompressible. Point of reference is localized in descending aorta.

5.1 Pressure

Obtained relative static pressure on the walls of domain is presented on contours, in two of characteristic points of cardiac cycle: systole (see Fig. 5.1) and diastole (see Fig 5.2). Highest pressure for about 6,8 kPa is localized on inlet of domain in systole (0.14s of calculation). In the same period of time the lowest pressure equal to -7.7 kPa is localized on CoA. Systolic pressure difference is equal to 14.5kPa. Diastolic maximum pressure was about 600 Pa on descending aorta outlet. The lowest diastolic pressure was noticed before CoA inlet, equals to - 2 kPa.

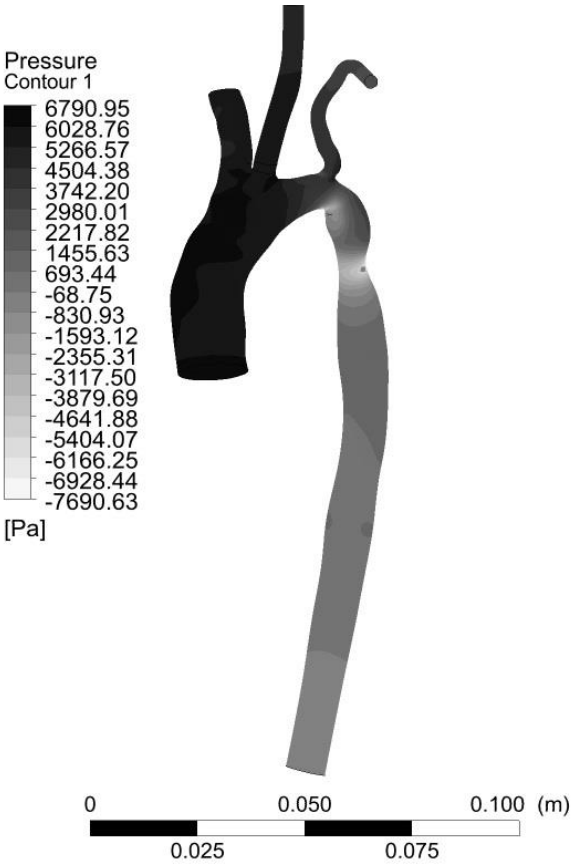

Fig.5.1. Contours of systolic static pressure

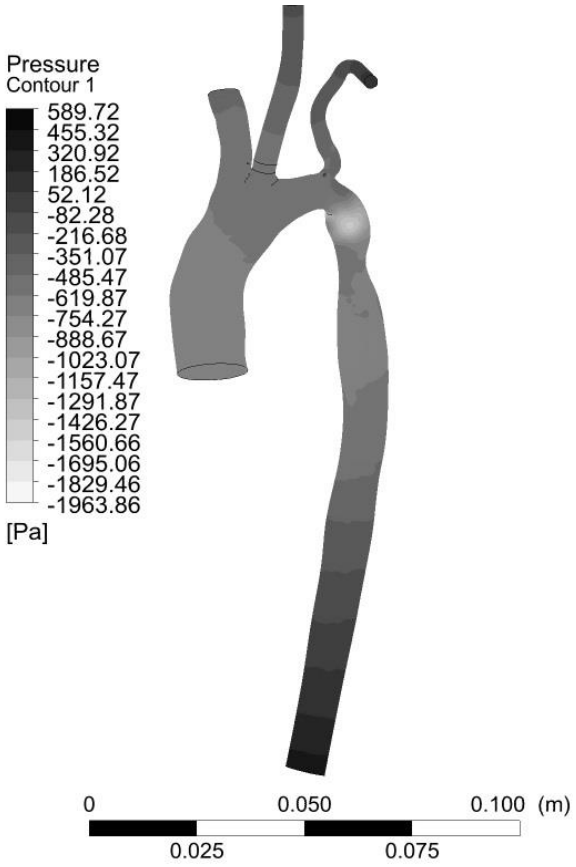

Fig.5.2. Contours of diastolic static pressure

5.2 Wall stress tensor

Plasma wall stress tensor of two characteristic points was presented inFig.5.3 and Fig. 5.4. The magnitude of about 260 Pa was obtained on aortic arch, on maximum angulation, before CoA. Noticeable magnification was located in CoA equal to 90Pa. Diastolic primary phase maximum wall stress tensor is located in the same part of aortic arch (Fig. 5.4) like in systolic cycle period, 43 Pa.

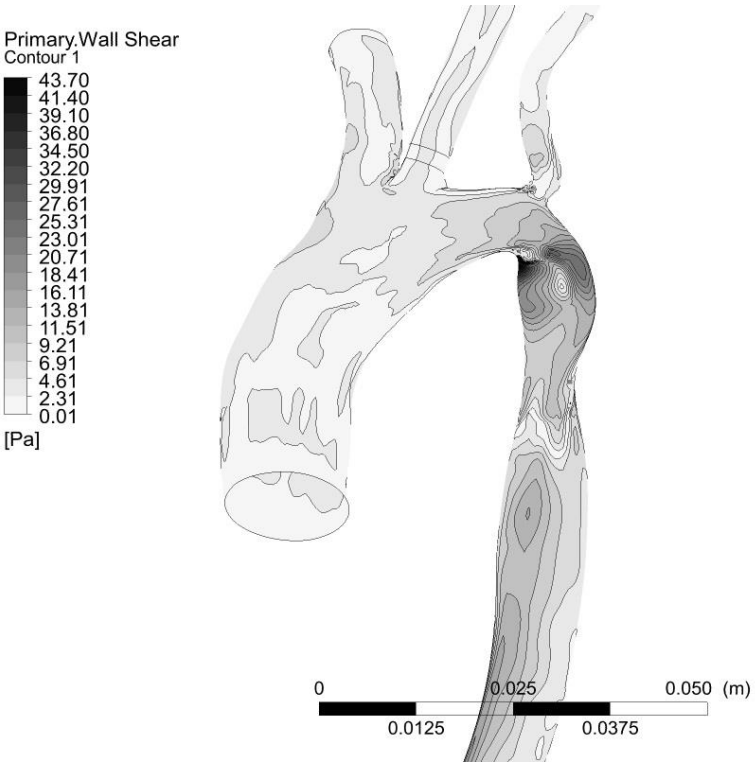

Fig.5.3. Primary phase diastolic wall shear stress

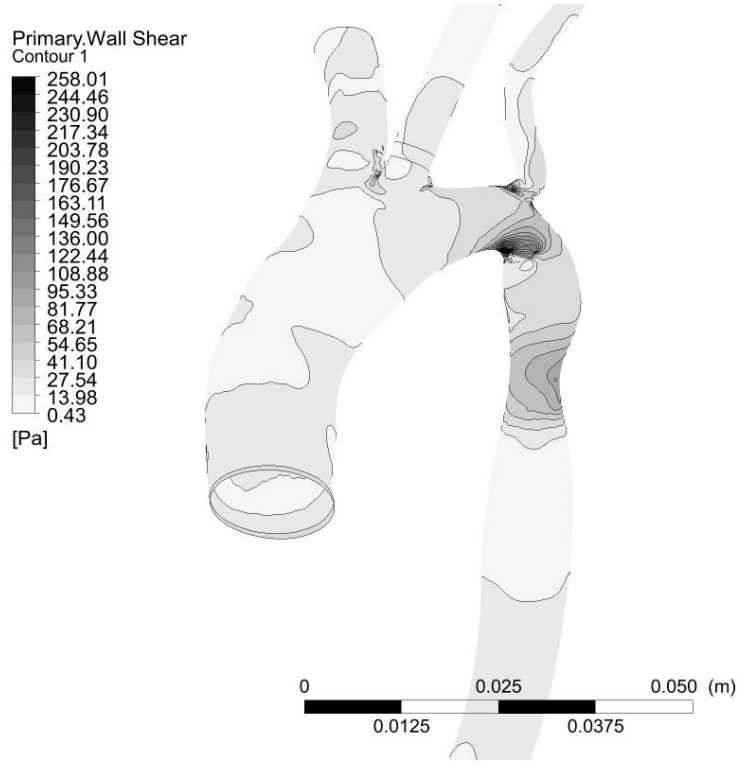

Fig.5.3. Primary phase systolic wall shear stress

Secondary phase (RBCs) distribution of wall stress tensors have comparable space distribution but vary with value: for systole (Fig. 5.5) it is 62 Pa and for diastole (Fig. 5.5) is 6 Pa.

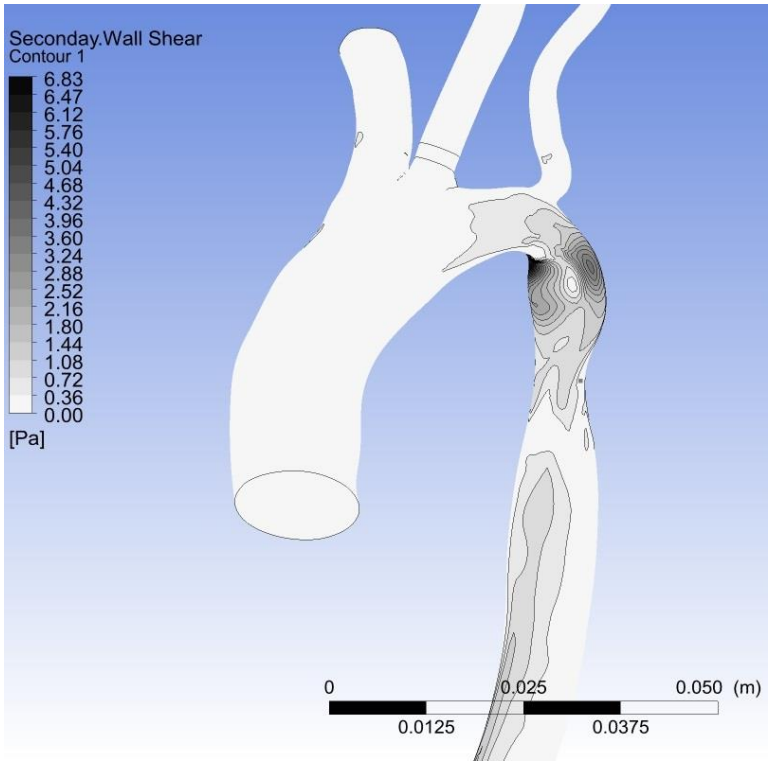

Fig.5.5. Secondary phase systolic wall shear stress

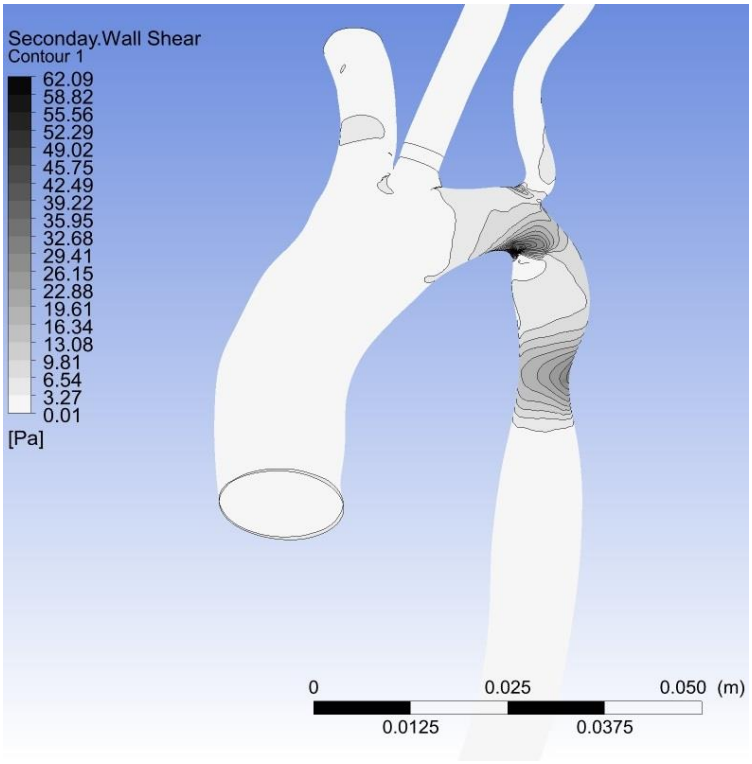

Fig.5.6. Secondary phase diastolic wall shear stress

Velocity

The highest velocity magnitude was obtained during systole on outflow from CoA (4,15 m/s), shown on velocity vectors (Fig. 5.7). Volume surrounding maximum velocity area shows also significantly increased velocity in narrowing cross section at aortic arch, before CoA. At diastole (Fig. 5.7), highest velocity magnitude occurs at aortic arch, equal to 1,44 m/s.

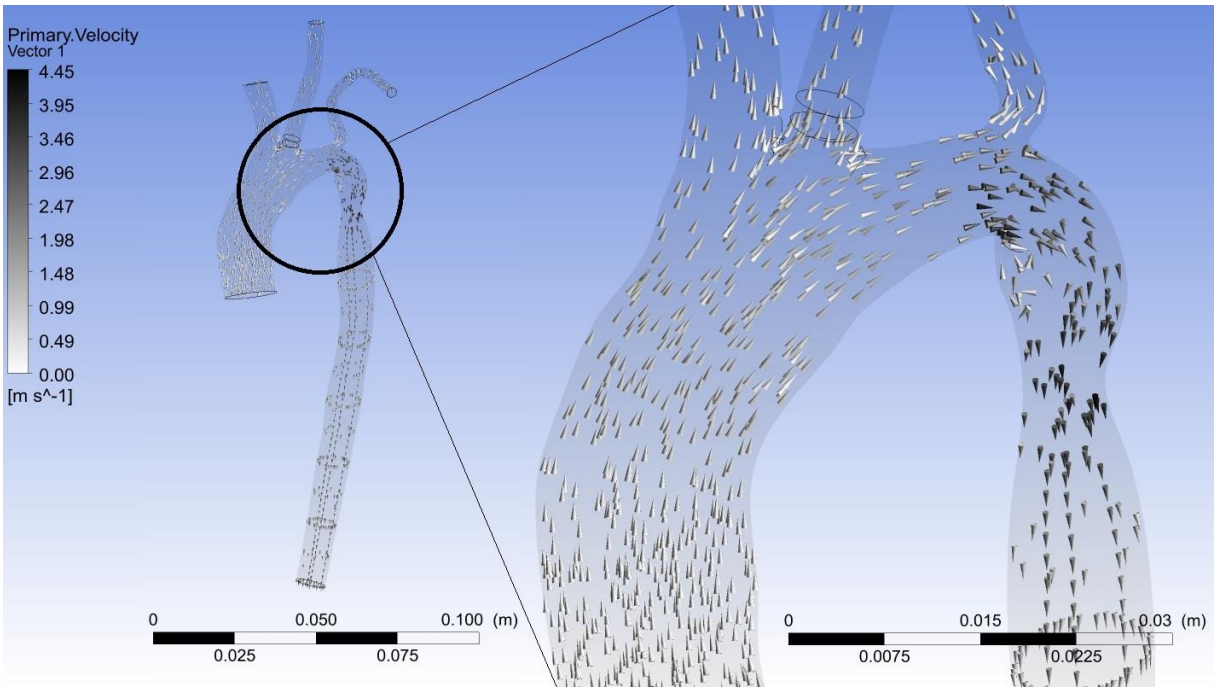

Fig.5.7. Vectors of systole with CoA (zoomed)

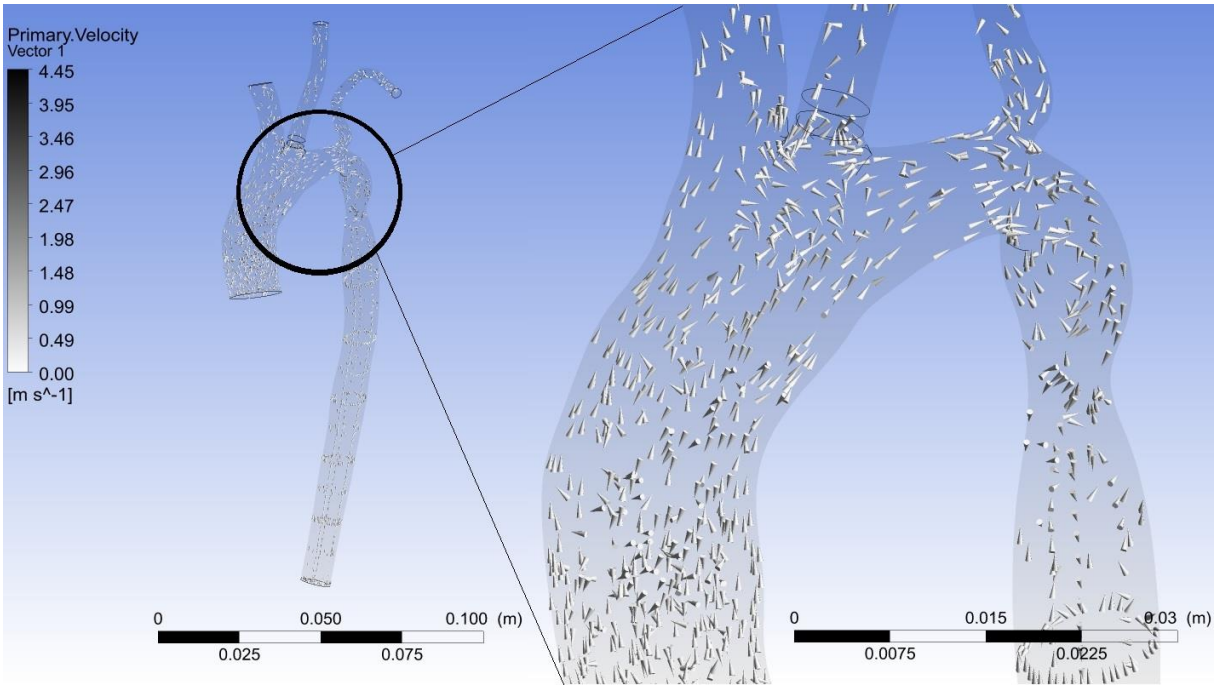

Fig.5.8. Vectors of diastole with CoA (zoomed)

5.3 Particles residence time

According to positions of tracked in Lagrangian reference frame partitions shown in (fig.5.9) is visible that particles eddy in domain due to turbulence caused by CoA. Part of (fig.5.9) where particles residence time of total flow time is 0.9 sec (beginning of second calculated cycle), shows that particles after first cardiac cycle still remains in domain reaching residence time near 0.9 sec.

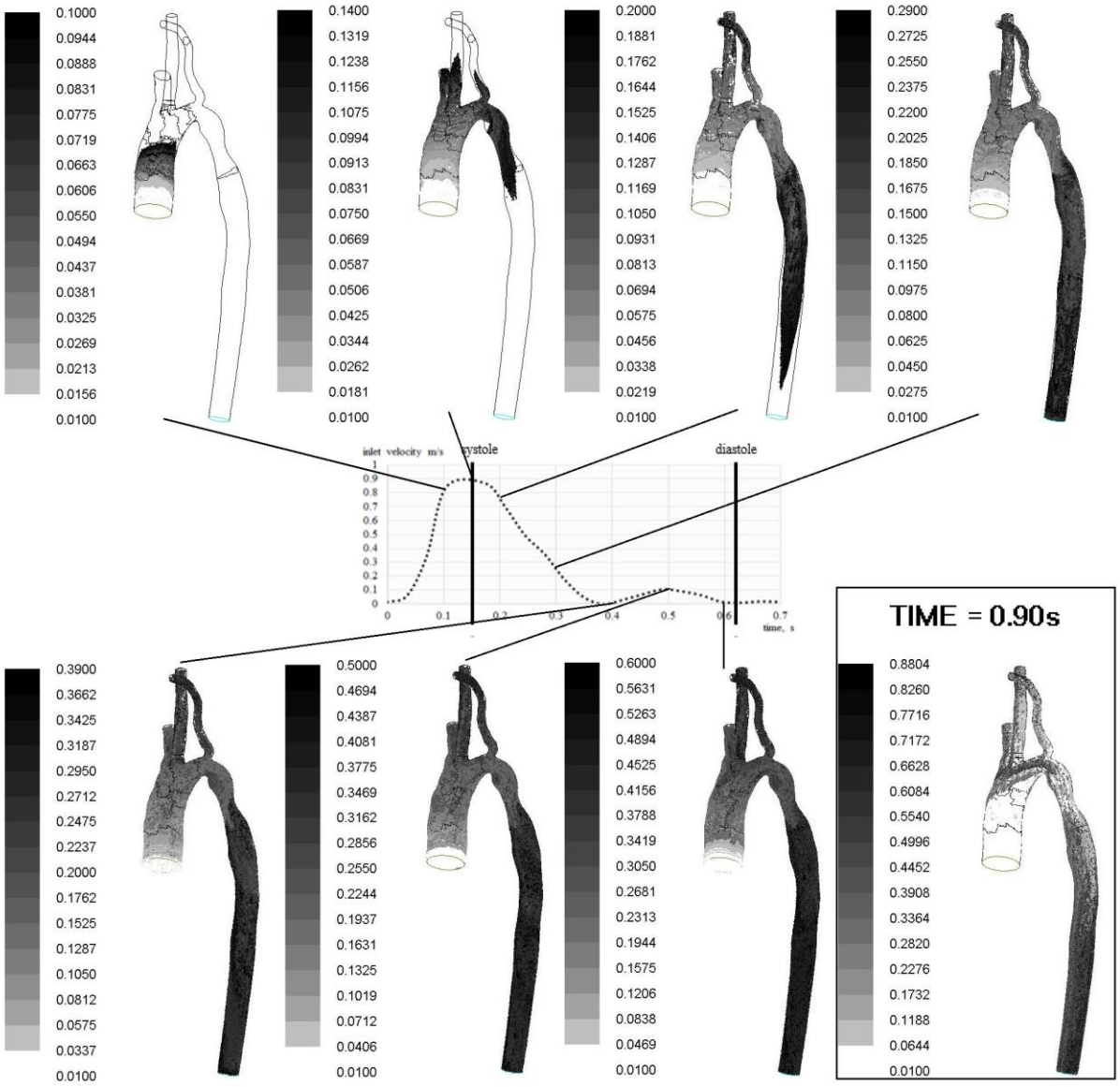

Fig.5.9. Particle residence time in chosen times of cardiac cycle

5.4 Diameter distribution

Particles diameter distribution in 0,7s of simulation (Fig.5.10) presents variety of diameter generated by EEDDM. Predominance of diameters near to 11 μm is noticeable due to assumed mean diameter on that level.

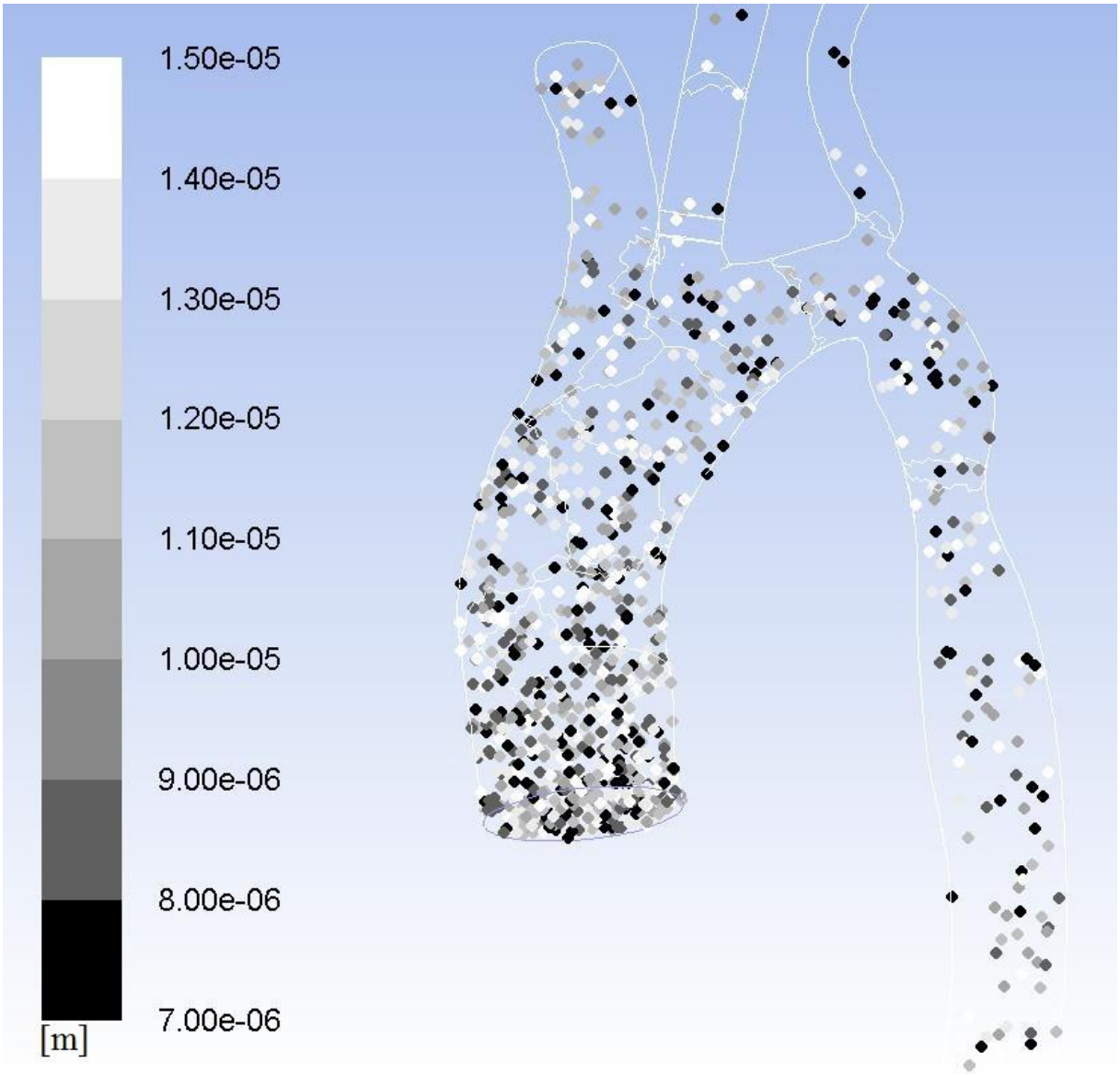

Fig.5.11. Particle Residence time in 0,7s of simulation

6. Conclusions

In presented work practical applications of CFD modeling was shown. Blood flow in 8 years old human female section of aorta and its main bifurcations was computed. Real geometry contains a congenital condition – Coarctation of the aorta (CoA), with about 65% of vasoconstriction. Two main calculation models was considered. Eulerian grid was used to calculate two main fractions of morphological elements in blood: Plasma and RBCs, when Lagrangian grid

was used to track particles of WBCs. Work shows blood velocity distribution, static pressure, wall share stress in two main cardiac cycle characteristic points (diastole and systole). The particle residence time of WBCs in domain was presented. Significant extension of time flow in domain was revealed due to eddy caused by CoA.

An innovative way of modeling blood flow includes in pioneering discipline which is bio-technology. Great labor input is undertaking to constant improving interdisciplinary approach, nevertheless there is still need of engage more different fields specialists to get a wider picture.

Acknowledgements

I would like to acknowledge all project group members: Bartlomiej Melka, Wojciech Adamczyk, Marek Rojczyk, for great time spent together during work on case, especially my thesis supervisor Dr Ziemowit Ostrowski. I would like also to thank Adam Golda and Andrzej J. Nowak for help and cooperation.

Literature:

[A] ANSYS, Inc. ANSYS Fluent. 2016. *htpp://www.ansys.com*

[C] CFD Challenge problem: http://www.vascularmodel.org/miccai2012 (accessed May 16th 2016).

[1] Wojciech P. Adamczyk, Adam Klimanek, Ryszard A. Białecki, Gabriel Węcel,Paweł Kozołub, Tomasz Czakiert, Comparison of the standard Euler–Euler and hybrid Euler–Lagrange approaches for modeling particle transport in a pilot-scale circulating fluidized bed, *Particuology* (2016).*Elsevier B.V.,*

[2] J. Ding and D. Gidaspow. A Bubbling Fluidization Model Using Kinetic Theory of Granular Flow *AIChE J.* (1990) **36**(4):523–538

[3] F. Durst, D. Milojevic, B. Schönung, Eulerian and Lagrangian predictions of particulate two phase flows: a numerical study, *Appl. Math. Modelling* (1984)**8**,

[4] S. Ergun. Fluid Flow through Packed Columns. *Chem. Eng. Prog.*(1952) **48**(2):89–94

[5] D. Gidaspow, R. Bezburuah, and J. Ding. *Hydrodynamics of Circulating Fluidized Beds, Kinetic Theory Approach*. In Fluidization VII, Proceedings of the 7th Engineering Foundation Conference on Fluidization. 75–82 (1992)

[6] D. Gidaspow, V. Chandra, Unequal granular temperature model for motion of platelets to the wall and red blood cells to the center, *Chemical Engineering Science* (2014) **117**: 107-113

[7] J. Górski, *Fizjologia człowieka*, Wydawnictwo lekarskie PZWL (2010)

[8] J. Tu, G. Heng Yeoh, C. Liu, *Computational Fluid Dynamics: A Practical Approach*, Butterworth-Heinemann, (2007)

[9] Jung J and Hassanien A., Three-phase CFD analytical modelling of blood flow, *Medical Engineering & Physics* **20**:91-103, 2008.

[10] S.J. Konturek, *Fizjologia czowieka*, ELSEVIER Urban & Partner, 2007

[11] B. E. Launder and D. B. Spalding. *Lectures in Mathematical Models of Turbulence*. Academic Press, London, England (1972)

[12] C. K. K. Lun, S. B. Savage, D. J. Jeffrey, and N. Chepurniy. Kinetic Theories for Granular Flow: Inelastic Particles in Couette Flow and Slightly Inelastic Particles in a General Flow Field. *J. Fluid Mech.*(1984) **140**:223–256

[13] F.D. Molina-Aiz, H. Fatnassi, T. Boulard, J.C. Roy, D.L. Valera, Comparison of finite element and finite volume methods for simulation of natural ventilation in greenhouses, *Computers and Electronics in Agriculture* (2010) **72**(2):69-86

[14] S. A. Morsi and A. J. Alexander. An Investigation of Particle Trajectories in Two-Phase Flow Systems. J. Fluid Mech. 55(2). 193–208. September 26 1972.

[15] Patankar N.A and Joseph D.D. Lagrangian numerical simulation of particulate flows. *International Journal of Multiphase Flow* (2001) **27**.

[16] A. Polanczyk, A. Piechota, CFD simulations of blood flow through abdominal part of aorta, *Challenges of modern technology* (2010) **1**

[17] W. Z. Traczyk, *Fizjologia człowieka w zarysie*, Wydawnictwo lekarskie PZWL, 2002.

[18] C.-Y. Wen and Y. H. Yu. Mechanics of Fluidization. *Chem. Eng. Prog. Symp. Series.* **62**. 100–111. 1966.

Identyfikacja oraz modelowanie procesu przepływu krwi w części dużego naczynia krwionośnego z wykorzystaniem wielofazowego modelu hybrydowego Euler-Lagrange

Słowa kluczowe: aorta, CFD, przepływ krwi, ANSYS Fluent, Euler-Lagrange, Euler-Euler, wielofazowy, DPM

Abstrakt

Obliczeniowa mechanika płynów (ang. CFD – Computational Fluid Dynamics) znana niegdyś tylko w wysoce wyspecjalizowanej technicznie branży jest jednym z podstawowych narzędzi inżynieryjnych w rozwiązywaniu wielu złożonych problemów, celem zdobycia kluczowych informacji i poszerzenia wiedzy ogólnej w wielu dziedzinach. CFD pozwala na tworzenie nowych, bardziej zaawansowanych systemów oraz na udoskonalanie już istniejących – poprawiając ich wydajność i/lub obniżając koszty produkcji oraz eksploatacji. Aktualna sytuacja wymaga od inżynierów zmierzenia się w trudnej dyscyplinie – walce o ułamki wydajności z powodu ograniczeń materiałowych i konstrukcyjnych. Przedsięwzięcia te nie koncentrują się jedynie na oczywistych dyscyplinach, takich jak przepływ ciepła, mechanika płynów czy wytwarzanie energii, ale także na nowych, niezbadanych sferach jak inżynieria motoryzacyjna, chemiczna, kosmiczna czy środowiska itd.

Jednym z innowacyjnych zastosowań CFD jest bio-inżynieria. W medycynie, symulacje komputerowe są w stanie dostarczyć niezbędnych, nierzadko ratujących życie informacji, bez ingerencji w ciało pacjenta (in vitro), co pozwala uniknąć późniejszych komplikacji, zagrożeń występujących w trakcie wprowadzania przyrządów w ciało pacjenta czy niebezpiecznych nieprzewidywalnych powikłań. Ponad to w wielu przypadkach metody in vivo są niemożliwe do zastosowania ze względu na zagrożenie życia pacjenta.

Głównym celem powyższego projektu było stworzenie i testy innowacyjnego, dokładnego modelu przepływu krwi w ludzkiej aorcie.

Aktualnie dostępne badania nie uwzględniają przestrzennych interakcji pomiędzy poszczególnymi fazami krwi i ścianami naczyń krwionośnych. Takie podejście zdecydowanie zmniejsza dokładność tego typu modeli. Odpowiednie badania wzbogacają wiedzę ogólną o dokładne informacje , które mogą okazać się kluczowe we wczesnym diagnozowaniu problemów układu sercowo-naczyniowego, wskazując na potencjalnie podatne obszary (np. kurczące się naczynia krwionośne). Tak dokładne informacje są trudno dostępne do uzyskania na drodze badań.

Poza wielofazowa koncepcją projektu, który rozpatruje każdy komponent krwi jako oddzielną fazę, przyporządkowując poszczególne właściwości do każdej z nich i uwzględniając ich wzajemne relacje, szczególną uwagę zwrócono na realistykę geometrii – zakładając rzeczywisty układ aortalny (część aorty wstępującej, łuk aortalny i część aorty zstępującej) uwzględniający bifurkację. Ponadto wprowadzono do modelu przepływ pulsacyjny za pomocą wbudowanej wewnętrznej funkcji programu. (ang. UDF – User Defined Function).